Published in final edited form as:
*Magn Reson Med*. 2014 October ; 72(4): 1049–1056. doi:10.1002/mrm.25024.

# Pseudocontinuous Arterial Spin Labeling with Prospective Motion Correction (PCASL-PROMO)

**Zungho Zun**[1,*], **Ajit Shankaranarayanan**[2], and **Greg Zaharchuk**[1]

[1]Department of Radiology, Stanford University, Stanford, California, USA

[2]Applied Science Laboratory, GE Healthcare, Menlo Park, California, USA

## Abstract

**Purpose—**Arterial spin labeling (ASL) perfusion imaging with a segmented three-dimensional (3D) readout is becoming increasing popular, yet conventional motion correction approaches cannot be applied in segmented imaging. The purpose of this study was to demonstrate the integration of 3D pseudocontinuous ASL (PCASL) and PROMO (PROspective MOtion correction) for cerebral blood flow measurements.

**Methods—**PROMO was integrated into 3D PCASL without increasing repetition time. PCASL was performed with and without PROMO in the absence of motion. The performance of PCASL-PROMO was then evaluated with controlled motions using separate scans with and without PROMO and also with random motion using an interleaved scan where every repetition time is repeated twice, once with and once without PROMO.

**Results—**The difference in the average ASL signal of the 3D volume between conventional and PROMO implementations was negligible (<0.2%). ASL image artifacts from both controlled and random motions were removed significantly with PROMO, showing improved correlation with reference images. Multiple combinations of data acquired using the interleaved scan revealed that PROMO with real-time motion updating alone reduces motion artifact significantly and that rescanning of corrupted segments is more critical in tagged images than control images.

**Conclusion—**This study demonstrates that PROMO is a successful approach to motion correction for PCASL cerebral blood flow imaging.

### Keywords

prospective motion correction; PROMO; arterial spin labeling; PCASL; ASL

## INTRODUCTION

Arterial spin labeling (ASL) is a noninvasive, non–contrast perfusion imaging method that has extensively been applied to measure cerebral blood flow (CBF). Its sensitivity to subject motion arises from the fact that ASL relies on the cancellation of static tissues in the subtraction between images with and without blood tagging, which are assumed to be



*Correspondence to: Zungho Zun, 1201 Welch Rd., Mailcode 5488, Stanford University, Stanford, CA 94305. zun@stanford.edu.

coregistered. Introduction of background suppression in ASL (1–3) has improved image quality greatly by reducing temporal noise partly stemming from motion. However, even with optimal background suppression, motion will still result in mis-registration of the location of perfusion information, which may manifest itself as blurring. Additionally, correcting for motion becomes more important for longer ASL acquisitions, such as might be acquired for higher resolution, transit time insensitivity, or resting state CBF imaging.

Prospective motion correction (4,5) is a technique based on updating pulse sequences in real time such that the logical coordinate system remains fixed with respect to the subject during the entire scan. Previous groups have reported on the use of retrospective motion correction for ASL using rigid-body image registration with or without discarding control/tagged image pairs that showed significant misregistration (6–10). Prospective motion correction based on a navigator has several advantages compared with these retrospective methods. First, the recent consensus in ASL community is toward 3D image acquisition for higher signal-to-noise ratio (SNR), and the navigator-based motion correction methods provide more flexibility in the 3D readout scheme. In other words, imaging acquisition is not limited to snapshot imaging (which acquires the whole imaging volume for each repetition time [TR]) but can be achieved in a segmented fashion. This enables shorter length of the individual interleaves and thus reduces the off-resonance artifacts in readout schemes such as 3D GRASE (11) or 3D stack-of-spiral. Second, prospective motion correction with a navigator is compatible with fully optimized background suppression. In motion correction based on ASL images themselves, background suppression is deliberately suboptimized to generate higher tissue contrast, especially in control images, and this in return not only reduces the ASL signal stability, but also incurs image artifacts in segmented image acquisition. Third, image registration based on tagged/control images is challenging compared with navigator images because these individual images have an extremely low SNR. Furthermore, because of background suppression, different contrast between tagged and control images requires complicated registration algorithms, such as ones with mutual information. The disadvantages of motion correction using navigators include possibly prolonged scan time due to the navigator sequence and potential perturbation to the primary imaging sequences.

PROMO (PROspective MOtion correction) is one method of image-based prospective motion correction and uses three orthogonal 2D navigator images with rigid-body tracking algorithm based on the extended Kalman filter (12). Compared with a k-space–based method, the image-based navigator provides the ability to define region of interest and thereby exclude nonrigid regions in the registration process. PROMO has demonstrated its effectiveness in pediatric imaging with high-resolution anatomical imaging (13,14) and in spectroscopy (15) and has shown compatibility with acceleration techniques (16). In this study, we demonstrate the incorporation of PROMO into pseudocontinuous ASL (PCASL) with a segmented 3D stack-of-spirals readout (17). The navigators are inserted within the ASL preparation time so that there is no increase in TR. We demonstrate that our integration of PROMO and PCASL does not affect the CBF measurement significantly, and leads to improved performance in the setting of both controlled and random motion. Preliminary versions of this work have been reported previously in abstract form (18,19).

# METHODS

## PCASL-PROMO Integration

Figure 1a shows our integration of PROMO and PCASL. In order to maintain the same TR as in PCASL without PROMO, the navigator block was incorporated into the time between saturation and inversion pulses in the ASL preparation, maintaining the same timing of preparation pulses as in PCASL without PROMO, at the potential risk of perturbing ASL imaging. The navigator itself was composed of three orthogonal two-dimensional images acquired in the axial, sagittal, and coronal planes, and was repeated three times. The example navigator images of three planes are shown in Figure 2. Because the amount of motion offset that can be tracked by one repetition of the navigator is limited, increasing the number of navigator repetitions for each TR provides more stable and faster motion correction; however, the number of repetitions is limited by the time interval of ASL preparation pulses, and, in principle, more repetition would lead to larger effects on the CBF measurement.

PROMO operates based on two correction features: *apply* and *rescan*. The navigator block in each TR produces six motion parameters, which are translations and rotations along the *x*, *y*, and *z* axes with respect to the reference position. *Apply* is the process of updating the coordinate system of the pulse sequence in each TR based on these motion parameters; *rescan* is the process of identifying the TRs during which a significant motion is suspected to have occurred in the imaging (based on comparison of the motion parameters before and after imaging) and repeating those TRs at the end of the scan to overwrite previous, presumably motion-corrupted data. Therefore, integration of PROMO into PCASL does not increase total scan time in the absence of motion, with the exception of time for the initial 20 successive navigators for the rigid-body region of interest defining process (9 s) (12). In our current integration, the update of the coordinate system only applies to the image acquisition, not the ASL labeling or background suppression pulses. Also, if a rescan of a corrupted TR is required, the structure of the sequence currently requires a pair of control/tagged images (2 TR) to be rescanned as one unit.

Figure 1b illustrates how *apply* and *rescan* work complementarily in PCASL-PROMO. If motion occurs during $TR_N$, then without PROMO, this would yield misregistration in the image acquisitions $IMG_N$, $IMG_{N+1}$, $IMG_{N+2}$, and so on. With PROMO, the motion is detected in the navigator $NAV_{N+1}$, and thereafter all the subsequent imaging ($IMG_{N+1}$, $IMG_{N+2}$ and so on) avoids misregistration caused by the motion offset from $TR_N$, by means of *apply*. However, the imaging segment of $IMG_N$ is still corrupted because this is performed before the navigator detects the motion. If the rescan metric of $TR_N$, which is L2 norm of difference between motion parameters of $NAV_N$ and $NAV_{N+1}$, is larger than a preset threshold, $TR_N$ is rescanned at the end to reacquire $IMG_N$. On the other hand, the maximum amount of motion that can be detected by one repetition of navigator is approximately 5 mm for translation and 5° for rotation, and with three repetitions of navigator in each TR, the maximum detectable motion in one TR is about 15 mm or 15°. If the amount of the motion exceeds this, the leftover motion continues to be tracked in the subsequent TRs. Until the motion is completely tracked, all the intermediate TRs are likely

to be flagged as segments to be rescanned depending on the rescan threshold. Finally, at the end of PCASL-PROMO scan (including rescanning), one last set of navigator is played to ensure that no significant motion occurred in the last TR (data not shown). Although PROMO can be applied to supplementary imaging such as proton density imaging required for CBF quantification and was used in this manner in our scans, our study focused on motion correction on ASL difference images.

### Disturbance to ASL CBF Measurement

Unlike PROMO integrated in anatomical imaging (12–14), in ASL the quantitative CBF measurement can be influenced by the placement of navigators in the dead time of ASL preparation. Some portion of upstream blood is perturbed by the sagittal/coronal plane excitation of the navigator, and the ASL signal change caused by this was found to be −1.4% in our simulation with a navigator flip angle of 8°. Because not all the upstream blood is excited by the navigator, the actual change in ASL signal would be much less than this. To verify that navigator does not alter the intrinsic CBF measurements, a PCASL scan was performed alternately with and without navigator (both without applying the motion parameters to track the brain) three times for each method in two normal volunteers who remained as still as possible.

### Controlled Motion Experiment

The performance of PCASL-PROMO was evaluated in the presence of controlled motion. Two representative types of motions were examined: side-to-side and nodding motion. PCASL was performed with and without PROMO in a volunteer who was instructed to perform controlled motions repeatedly during the scans. Reference images were acquired using PCASL without PROMO in the same volunteer without any intended motion.

### Random Motion with Interleaved Scan Experiment

To explore more realistic and comprehensive motions, PCASL-PROMO was performed in the presence of random pattern of motions in this experiment. Because random motions cannot be repeated the same way in two separate scans, we implemented an interleaved PCASL-PROMO sequence where every TR is repeated twice with and without PROMO, leading to a doubled scan time (20). This scan was performed in five volunteers (1 female, ages 37 ± 5 years). Each volunteer was instructed to move their head in random directions at random timing during the entire interleaved scan. The interleaved scan sequences save all the data separately; data without any correction, data acquired with the updating of the coordinate system based on the measured motion parameters, and rescanned data. Tagged and control images were also saved separately. The separate storage of the data enabled reconstruction using multiple combinations of the datasets. We reconstructed 1) ASL images without PROMO, 2) ASL images with *apply* only, 3) ASL images with PROMO (both *apply* and *rescan*), 4) ASL images with rescanning tagged images only, and 5) ASL images with rescanning control images only. This analysis investigated the benefit of *rescan* and its effect on tagged and control images separately. This is important, because each rescanned TR will add time to the sequence, which may not be preferred in certain time-sensitive applications. Reference ASL images were also acquired without PROMO in the absence of

any intended motion. Reference scan was performed twice to provide comparison of correlation between two reference scans and that between reference and PROMO scans.

### Image Analysis

Images from each coil element were combined using optimal B1 reconstruction (OBR) (21,22) with coil sensitivity maps that were acquired from proton density images. Optimal B1 reconstruction provides accurate measurements, particularly when the signal amplitude is close to zero, which is the case with ASL signal in white matter, and thus provides better gray matter/white matter contrast in ASL images. Reconstructed images were coregistered to the reference ASL images, and then Pearson's correlation coefficients were calculated for each slice and for the whole 3D volume, with respect to the reference ASL images to evaluate the accuracy of motion correction. Pearson's correlation was employed rather than sum-of-squares because there may exist a temporal variation of global CBF due to physiological change. All image analyses/registrations were performed using MAT-LAB (Mathworks, Inc., Natick, Massachusetts, USA) and SPM8 (Wellcome Trust Center for NeuroImaging, University College London, London, UK).

### Experimental Setup

Image acquisition in PCASL was performed using fast-spin echo 3D stack of spiral imaging with eight interleaves. Imaging parameters were TE = 10.6 ms, TR = 4.8 s, spiral readout time = 4.1 ms, spatial resolution = $3.4 \times 3.4 \times 4.0$ mm$^3$, FOV = $220 \times 220 \times 144$ mm$^3$, 36 slices, labeling duration = 1450 ms, and postlabeling delay = 2025 ms. Background suppression was achieved in all scans using one saturation and five inversion pulses at 4322 ms, 3510 ms, 2005 ms, 903 ms, 325 ms, and 73 ms prior to image acquisition, respectively. The saturation and the first inversion were slab-selective pulses applied onto the imaging volume and were played before tagging pulses while the other inversions were near-nonselective and were applied after tagging pulses. The number of averages was three for all scans except for the interleaved scan experiment, which used two averages. Corresponding total scan times were 4:30 min and 6:15 min, respectively, without rescanning. In PROMO, navigator images were acquired using a single-shot spiral gradient echo sequence using the following parameters: flip-angle = 8°, TE = 0.8 ms, spiral readout time = 8.2 ms, spatial resolution = 9.2 × 9.2 mm, FOV = 320 mm, and slice thickness = 13 mm. Three sets of navigators were played leading to a duration of 628 ms for the navigator block in each TR. All scans were performed on a GE MR750 3T scanner, and all volunteers provided written consent under an institutional policy.

## RESULTS

### Disturbance to ASL CBF Measurement

Figure 3 contains the results of six PCASL scans performed alternately with and without navigator excitation for each volunteer. Each data point in Figure 3 corresponds to the average ASL signals of the 3D volume for each scan normalized by the average across the scans for each volunteer. Volunteer 1 showed temporal fluctuation of ASL signal, whereas the signal increased monotonically over time in volunteer 2. The average ASL signal with

navigator was 0.2% higher than ASL signal without navigator, indicating negligible change in ASL measurement due to navigator excitation.

### Controlled Motion Experiment

Figure 4 contains the motion parameters that were recorded during the scans with side-to-side and nodding motions. The dominant change in motion parameters was rotation along the *z*-axis (superior–inferior) for side-to-side motion, and rotation along the *x*-axis (left–right) for nodding motion as expected. Figure 5 compares the reference ASL images (acquired without PROMO and without intended motion) and ASL images with and without PROMO for each motion type. For side-to-side motion, ASL images without PROMO showed significant blurring due to motion, whereas this was reduced greatly with PROMO. For nodding motion, there was no significant visible difference between ASL images with and without PROMO, except that there was slight blurring in the superior slices without PROMO. Figure 6 shows Pearson correlation coefficients calculated for each slice between the reference images and the ASL images with or without PROMO for each motion type. ASL images with PROMO for both motion types showed consistent correlation with the reference images. ASL images without PROMO in the presence of side-to-side motion showed far reduced correlation as expected from the blurred images. ASL images without PROMO in the presence of nodding motion showed lower correlation in the superior and inferior slices, as larger motion offsets are expected in these slices in axial imaging with nodding. Table 1 summarizes the average correlation coefficients and average CBF for each case.

### Random Motion with Interleaved Scan Experiment

Figure 7 shows the motion parameters saved during the interleaved scan in one representative volunteer with random motion. Although the subjects were instructed to move randomly, the two most dominant motions were rotations along the *z*-axis and *x*-axis that correspond to side-to-side and nodding motions in all volunteers. Corresponding ASL images reconstructed from multiple combinations of the data are displayed in Figure 8. While the images without PROMO (second row) showed severe blurring due to random motion, the blurring was reduced dramatically using PROMO (sixth row). The blurring was also reduced significantly using *apply* only (third row). The fourth and fifth rows in Figure 8 show ASL images with *apply* on both tagged and control images but with rescanning either tagged or control images only. While images with rescanning control images only showed no significant visible difference from the images with *apply* only, images with rescanning tagged images only showed considerable reduction of blurring and exhibited image quality close to the images with full PROMO correction. Correlation coefficients calculated between these ASL images of each method and the reference images confirm the visual inspection as shown in Figure 9. Figure 9 also shows the correlation coefficients between two reference ASL images to provide the reference for the correlation coefficients. Table 2 summarizes the mean ± standard deviation (SD) across the subjects of the correlation coefficients between 3D ASL images of each reconstruction method and the first reference ASL images and the mean ± SD of global CBF measurements in gray matter. The *P* values were calculated using a *t* test with respect to the second reference scans. Although there was no significant visual difference between the second reference and PROMO ASL images,

there was a statistically significant difference in correlation coefficient ($P = 0.036$). In contrast, there was no statistically significant difference in CBF measurement between the reference scan and random motion scan with any reconstruction method.

## DISCUSSION

This study demonstrates the integration of PCASL and PROMO for prospective motion correction in CBF measurement. In particular, this method can be applied to segmented 3D readout schemes, which are becoming the standard for ASL due to superior SNR and reduced susceptibility artifacts. Such a method enables longer acquisitions to be acquired, as might be required for higher-resolution CBF imaging, acquisitions with very long postlabel delays (to provide insensitivity to arterial arrival time), or for resting-state CBF imaging.

PCASL-PROMO showed considerable reduction of motion artifacts caused by controlled motions such as side-to-side and nodding head motions. Side-to-side motion appeared to generate more blurring in our ASL images. This is because side-to-side motion is more prominent than nodding motion in an axial plane, as vice versa is expected in a sagittal plane, and also because there is more room for side-to-side motion in the head coil. For far superior and inferior axial slices, however, nodding motion yielded nonnegligible misregistration as shown in Figure 6 because of larger offset at the furthest locations from the rotation center. PCASL-PROMO also showed robust performance in the presence of random motion. The interleaved scan enabled various combinations of data with and without PROMO. Comparison of these multiple reconstructions demonstrated that PROMO with real-time updating of the coordinate system (*apply*) alone can reduce the motion artifacts significantly and that tagged images may be prioritized in rescanning rather than control images if the time for rescanning is limited. Pearson's correlation coefficient was used as a metric for motion correction in this study. The correlation coefficient of reference-to-PROMO scans was still lower than that of reference-to-reference scans. However, the discrepancy may be reduced with a lower rescan threshold at the cost of increased rescanning time. Also, the correlation coefficients were lower with random motion compared with controlled motion due to lower SNR, because the number of averages was lower in the ASL scan with random motion (two versus three). The motions performed here (both controlled and random) are not natural motions and may be larger translations/rotations than the average motions from patient populations, but this demonstrates the performance of PCASL-PROMO even in extreme cases of large and persistent motions.

Currently, real-time updating of the coordinate system is only applied to image acquisition, not to ASL preparation including blood tagging partly because tagging location is rather far from rigid part of the brain where motion parameters are estimated. Given that there was no statistically significant difference in the average CBF measurement of 3D volume between the PCASL scans with and without motion ($P = 0.606$), it can be inferred that tagging efficiency was not significantly compromised by motion. Although demonstrated with PCASL, PROMO motion estimation is based on the 3D navigator module, which is independent of the ASL module and thus can be combined with other types of tagging schemes as well as other image acquisitions.

The only major expense for PROMO is the extra time for rescanning. However, ASL images reconstructed with and without rescanned data suggest that PROMO with *apply* only, which costs no extra time for rescanning, still leads to improved ASL images in the presence of these extreme motions. In our experiment with less frequent motion, images reconstructed with *apply* only were found to be even closer to the images with full PROMO correction, whereas images without any motion correction at all showed similar blurring to those with more frequent motion (data not shown). This is because the number of segments to be rescanned is roughly proportional to the number of motion occurrences, whereas the number of segments to benefit from *apply* is similar whether motion is frequent or not. Therefore, PROMO with *apply* only could be expected to provide adequate performance of motion correction in patient populations, without increased scan time.

If a user chooses to include rescanning in PCASL-PROMO, total rescanning time can be controlled by adjusting the threshold for rescan metric and/or the maximum number of TRs to be rescanned. That is, rescanning is performed for a predetermined number of tagged/control image pairs with the highest rescan metric (most motion). However, more efficient rescan schemes can be developed for a given rescanning time. One possible method is to use the contrast difference between tagged and control images. As shown in Figures 8 and 9, rescanning is more beneficial in tagged images because control images have very little contrast due to background suppression. Thus, rescanning tagged images may only be more time-efficient, or more generally, the rescan threshold can be set differently for tagged and control images. Discarding images rather than rescanning is also an option because there are typically multiple averages in ASL scans and less signal averages may be better than including misregistered images in the signal averaging. Another time-efficient rescan method would be smart rescanning; for example, if a tagged image from one pair and a control image from another pair are corrupted by two separate motions, only one pair of tagged/control images rather than two pairs can be rescanned to overwrite those images. Lastly, because side-to-side motion leads to more prominent blurring in an axial imaging plane that is commonly used in brain ASL, rotation along the *z*-axis can have higher weighting in rescan metric calculation. All of these methods are compatible with each other and can be combined to generate various rescan schemes. One caveat exists, however, when tagged/control pairs are not rescanned as one unit. In ASL, the signal level in individual tagged or control images can drift with low temporal frequency (23,24). This signal drift is mostly removed by subtraction of consecutively acquired tagged/control image pair. With either tagged or control images only acquired in rescanning, or with a long interval between tagged and control images in a matched pair, the signal drift can cause an error in ASL signal. Rescan schemes must be designed with this consideration.

In future work, PCASL-PROMO should be validated in aged, pediatric, and/or patient populations. Patients with dementia, seizures, tremor, or cough may also benefit. Another future direction would be more efficient integration of PCASL and PROMO in terms of pulse sequence timing. It may be more effective to place the navigator immediately prior to image acquisition. This is true if PROMO is performed only with *apply* because there is less chance of motion occurring between navigator and imaging, leading to fewer corrupted imaging segments. However, if *rescan* is performed, there is no significant benefit from a

closer navigator because rescanning still has to be performed for the imaging segment between two navigator blocks that show difference. In order to reduce the amount of unnecessary rescanning, the navigator should be placed twice for each TR, immediately before and after image acquisition. Despite this advantage, it may be difficult to find an interval long enough for navigator block immediately before imaging, avoiding background suppression pulses.

PROMO may be combined with ASL sequences for organs other than the brain. This would require new atlas of the organs, as PROMO uses a pre-entered brain atlas for image registration. In ASL for lung or kidney, the primary motion would be from respiration. The current interval between navigator blocks, which is the same as TR (4.9 s), is probably too long compared with the period of respiratory motion. Navigators immediately before and after image acquisition would be required in these applications to detect high-frequency motion. In myocardial ASL, it is more challenging to use PROMO due to cardiac pulsation in addition to respiration. Cardiac motion has even faster temporal frequency and also incurs nonrigid body motion. PROMO may be beneficial in myocardial ASL when used together with cardiac and respiratory gating.

## CONCLUSION

This study demonstrates the feasibility of PCASL combined with PROMO. The data shown here provide evidence that a substantial amount of motion artifacts are removed with PROMO, whereas the excitation of the navigator does not affect the intrinsic CBF measurement significantly. Future work should include validation of PCASL-PROMO in relevant patient populations.

## REFERENCES

1. Ye FQ, Frank JA, Weinberger DR, McLaughlin AC. Noise reduction in 3D perfusion imaging by attenuating the static signal in arterial spin tagging (ASSIST). Magn Reson Med. 2000; 44:92–100. [PubMed: 10893526]
2. St Lawrence KS, Frank JA, Bandettini PA, Ye FQ. Noise reduction in multi-slice arterial spin tagging imaging. Magn Reson Med. 2005; 53:735–738. [PubMed: 15723412]
3. Garcia DM, Duhamel G, Alsop DC. Efficiency of inversion pulses for background suppressed arterial spin labeling. Magn Reson Med. 2005; 54:366–372. [PubMed: 16032674]
4. Haacke EM, Patrick JL. Reducing motion artifacts in two-dimensional Fourier transform imaging. Magn Reson Imaging. 1986; 4:359–376. [PubMed: 3669950]
5. Lee CC, Jack CR Jr, Grimm RC, Rossman PJ, Felmlee JP, Ehman RL, Riederer SJ. Real-time adaptive motion correction in functional MRI. Magn Reson Med. 1996; 36:436–444. [PubMed: 8875415]
6. Luh WM, Wong EC, Bandettini PA, Hyde JS. QUIPSS II with thin-slice periodic saturation: a method for improving accuracy of quantitative perfusion imaging using pulsed arterial spin labeling. Magn Reson Med. 1999; 41:1246–1254. [PubMed: 10371458]
7. Petersen ET, Lim T, Golay X. Model-free arterial spin labeling quantification approach for perfusion MRI. Magn Reson Med. 2006; 55:219–232. [PubMed: 16416430]
8. Deibler AR, Pollock JM, Kraft RA, Tan H, Burdette JH, Maldjian JA. Arterial spin-labeling in routine clinical practice. Part 1: technique and artifacts. Am J Neuroradiol. 2008; 29:1228–1234. [PubMed: 18372417]

9. Wang Z, Aguirre GK, Rao H, Wang J, Fernandez-Seara MA, Childress AR, Detre JA. Empirical optimization of ASL data analysis using an ASL data processing toolbox: ASLtbx. Magn Reson Imaging. 2008; 26:261–269. [PubMed: 17826940]
10. Wu WC, Edlow BL, Elliot MA, Wang J, Detre JA. Physiological modulations in arterial spin labeling perfusion magnetic resonance imaging. IEEE Trans Med Imaging. 2009; 28:703–709. [PubMed: 19150788]
11. Oshio K, Feinberg DA. GRASE (Gradient- and spin-echo) imaging: a novel fast MRI technique. Magn Reson Med. 1991; 20:344–349. [PubMed: 1775061]
12. White N, Roddey C, Shankaranarayanan A, Han E, Rettmann D, Santos J, Kuperman J, Dale A. PROMO: real-time prospective motion correction in MRI using image-based tracking. Magn Reson Med. 2010; 63:91–105. [PubMed: 20027635]
13. Brown TT, Kuperman JM, Erhart M, White NS, Roddey JC, Shankaranarayanan A, Han ET, Rettmann D, Dale AM. Prospective motion correction of high-resolution magnetic resonance imaging data in children. Neuroimage. 2010; 53:139–145. [PubMed: 20542120]
14. Kuperman J, Brown T, Ahmadi M, Erhart M, White N, Roddey J, Shankaranarayanan A, Han E, Rettmann D, Dale A. Prospective motion correction improves diagnostic utility of pediatric MRI scans. Pediatr Radiol. 2011; 41:1578–1582. [PubMed: 21779892]
15. Keating B, Deng W, Roddey JC, White N, Dale A, Stenger VA, Ernst T. Prospective motion correction for single-voxel 1H MR spectroscopy. Magn Reson Med. 2010; 64:672–679. [PubMed: 20806374]
16. Banerjee S, Beatty PJ, Zhang JZ, Shankaranarayanan A. Parallel and partial Fourier imaging with prospective motion correction. Magn Reson Med. 2013; 69:421–433. [PubMed: 22488750]
17. Dai W, Garcia D, de Bazelaire C, Alsop DC. Continuous flow-driven inversion for arterial spin labeling using pulsed radio frequency and gradient fields. Magn Reson Med. 2008; 60:1488–1497. [PubMed: 19025913]
18. Zhang, J.; Zaharchuk, G.; Moseley, M.; Han, E.; White, N.; Roddey, C.; Rettmann, D.; Dale, A.; Kuperman, J.; Shankaranarayanan, A. Pulsed Continuous Arterial Spin Labeling (PCASL) with Prospective Motion Correction (PROMO). Proceedings of the 18th Annual Meeting of ISMRM; 2010; Stockholm, Sweden. Abstract 5034.
19. Zun, Z.; Shankaranarayanan, A.; Zaharchuk, G. Pseudocontinuous Arterial Spin Labeling with Prospective Motion Correction (PCASL-PROMO). Proceedings of the 21st Annual Meeting of ISMRM; 2013; Salt Lake City, Utah, USA. Abstract 3031.
20. Schulz J, Siegert T, Reimer E, Labadie C, Maclaren J, Herbst M, Zaitsev M, Turner R. An embedded optical tracking system for motion-corrected magnetic resonance imaging at 7T. Magn Reson Mater Phy. 2012; 25:443–453.
21. Roemer PB, Edelstein WA, Hayes CE, Souza SP, Mueller OM. The NMR phased array. Magn Reson Med. 1990; 16:192–225. [PubMed: 2266841]
22. Graves MJ, Emmens D, Lejay H, Hariharan H, Polzin J, Lomas DJ. T2 and T2* quantification using optimal B1 image reconstruction for multicoil arrays. J Magn Reson Imaging. 2008; 28:278–281. [PubMed: 18581394]
23. Aguirre GK, Detre JA, Zarahn E, Alsop DC. Experimental design and the relative sensitivity of BOLD and perfusion fMRI. Neuroimage. 2002; 15:488–500. [PubMed: 11848692]
24. Liu TT, Wong EC. A signal processing model for arterial spin labeling functional MRI. Neuroimage. 2005; 24:207–215. [PubMed: 15588612]

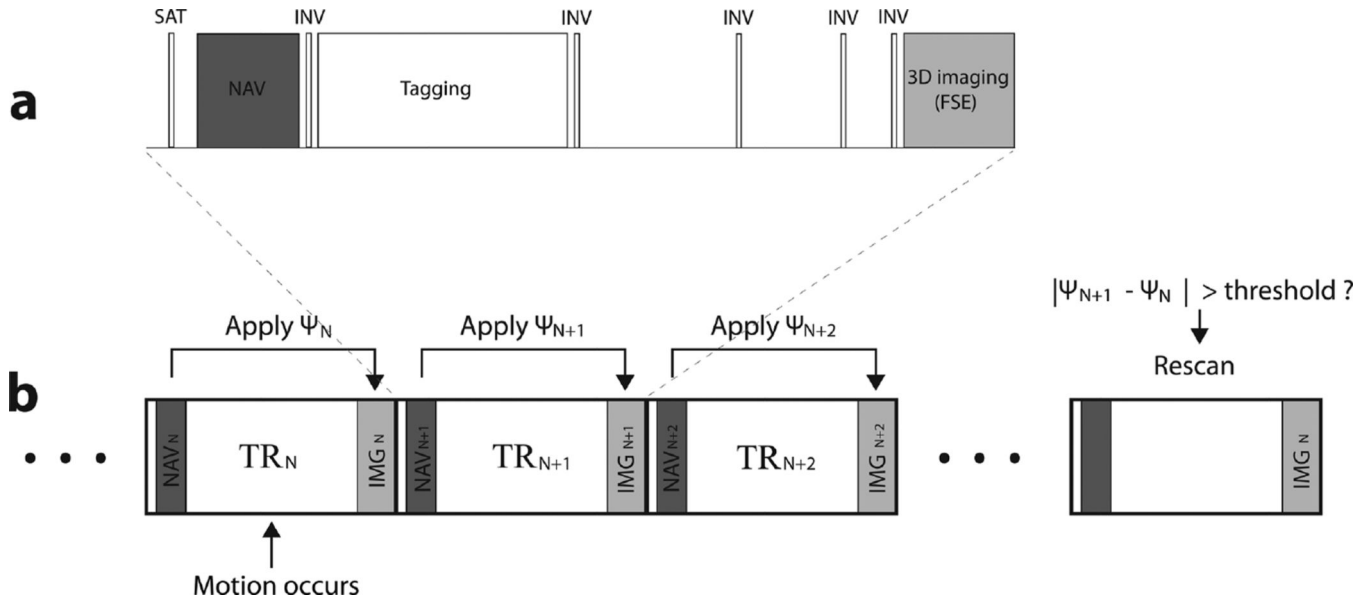


**FIG. 1.**

Illustration of integration of PCASL and PROMO in one TR (**a**) and the overall scan (**b**). The navigator is incorporated into ASL preparation without increasing TR. When motion occurs in $TR_N$, the image acquisitions $IMG_N$, $IMG_{N+1}$, $IMG_{N+2}$, and so on, will be misregistered without PROMO. Using PROMO, the motion is detected by $NAV_{N+1}$ and all the subsequent imaging ($IMG_{N+1}$, $IMG_{N+2}$, and so on) is corrected by applying motion parameters $\psi$ for pulse sequence update, although $IMG_N$ remains corrupted. If desired, the motion corrupted imaging $IMG_N$ can be rescanned at the end of the scan depending on the change of $\psi$.

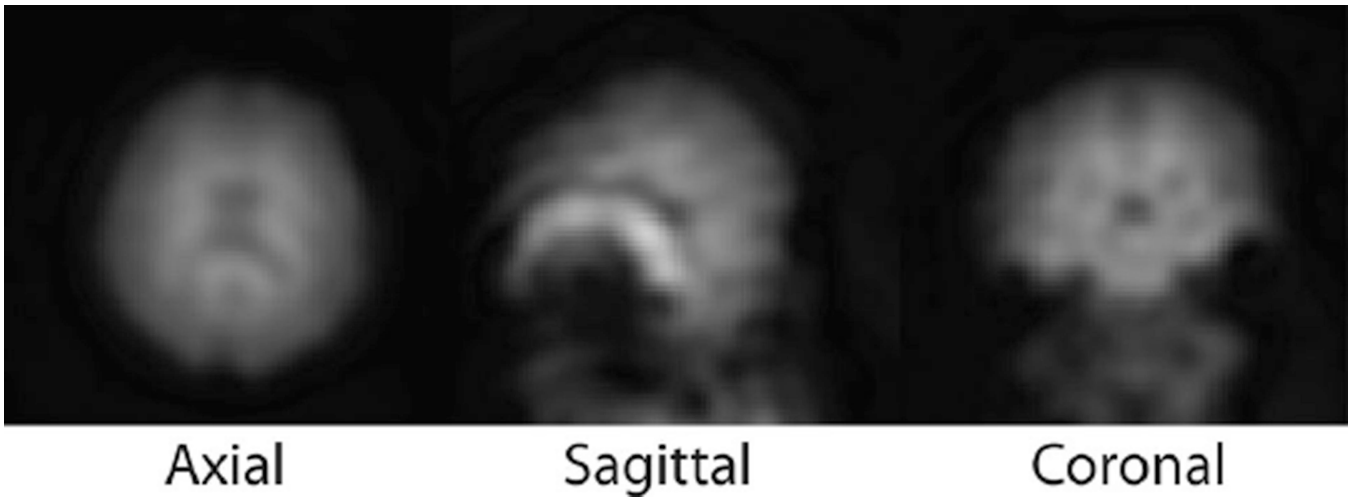


**FIG. 2.**

Example of low-resolution navigator images of three planes acquired in PCASL-PROMO scan using a single-shot spiral gradient echo sequence with a flip angle of 8° and a spatial resolution of 9.2 × 9.2 mm.

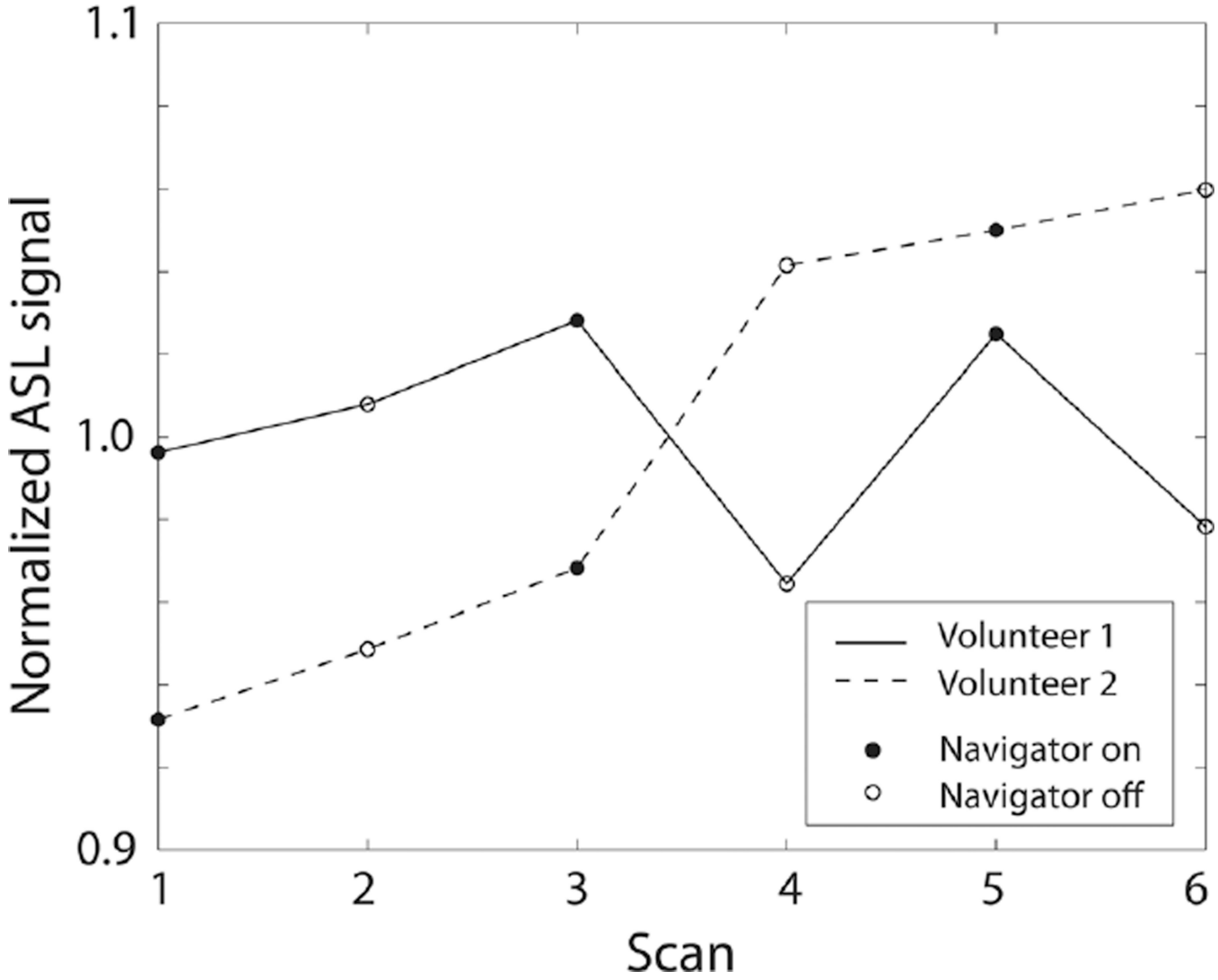


**FIG. 3.**

Average ASL signal of 3D volume measured in two volunteers using PCASL that was performed alternately with and without navigator excitation. Both volunteers remained as still as possible during the scans, and no motion correction was performed even when navigator was played. Average ASL signal with navigator was only 0.2% higher than average ASL signal without navigator.

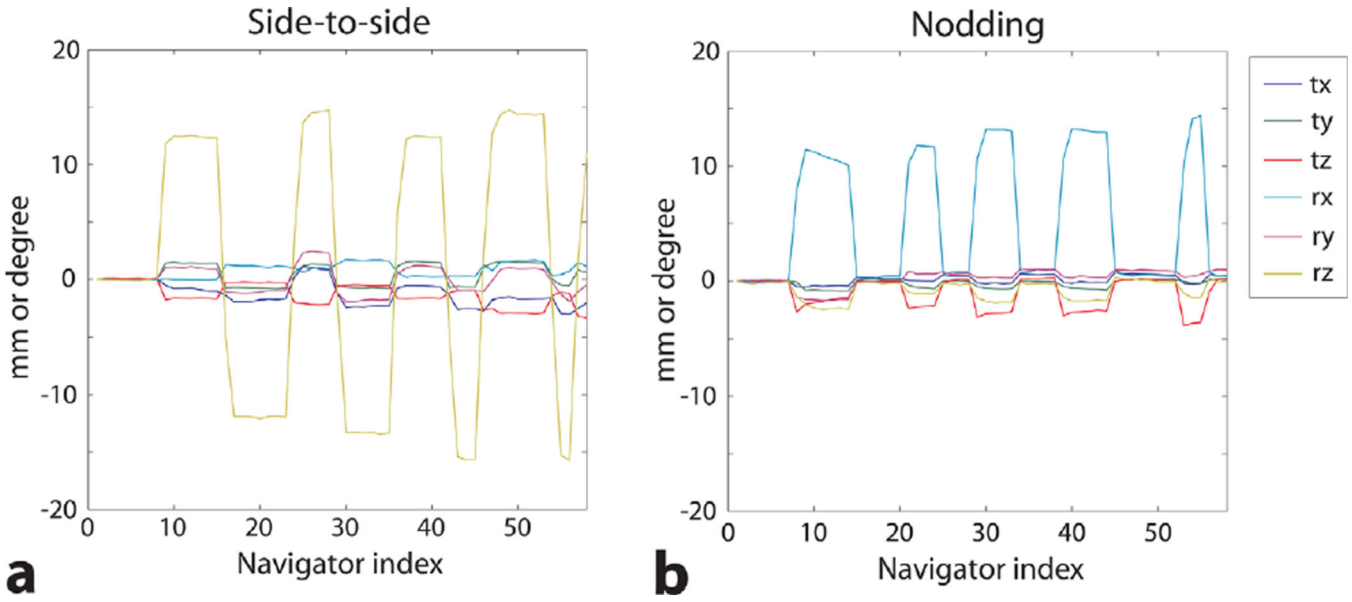


**FIG. 4.**

Motion parameters recorded by the navigators during scans in a volunteer with controlled motions. **a:** Side-to-side motion. **b:** Nodding motion. The notations tx, ty, tz, rx, ry, and rz correspond to translation (in millimeters) and rotation (in degrees) along the *x*- (left-right), *y*- (anterior–posterior) and *z*- (superior–inferior) axes. [Color figure can be viewed in the online issue, which is available at wileyonlinelibrary.com.]

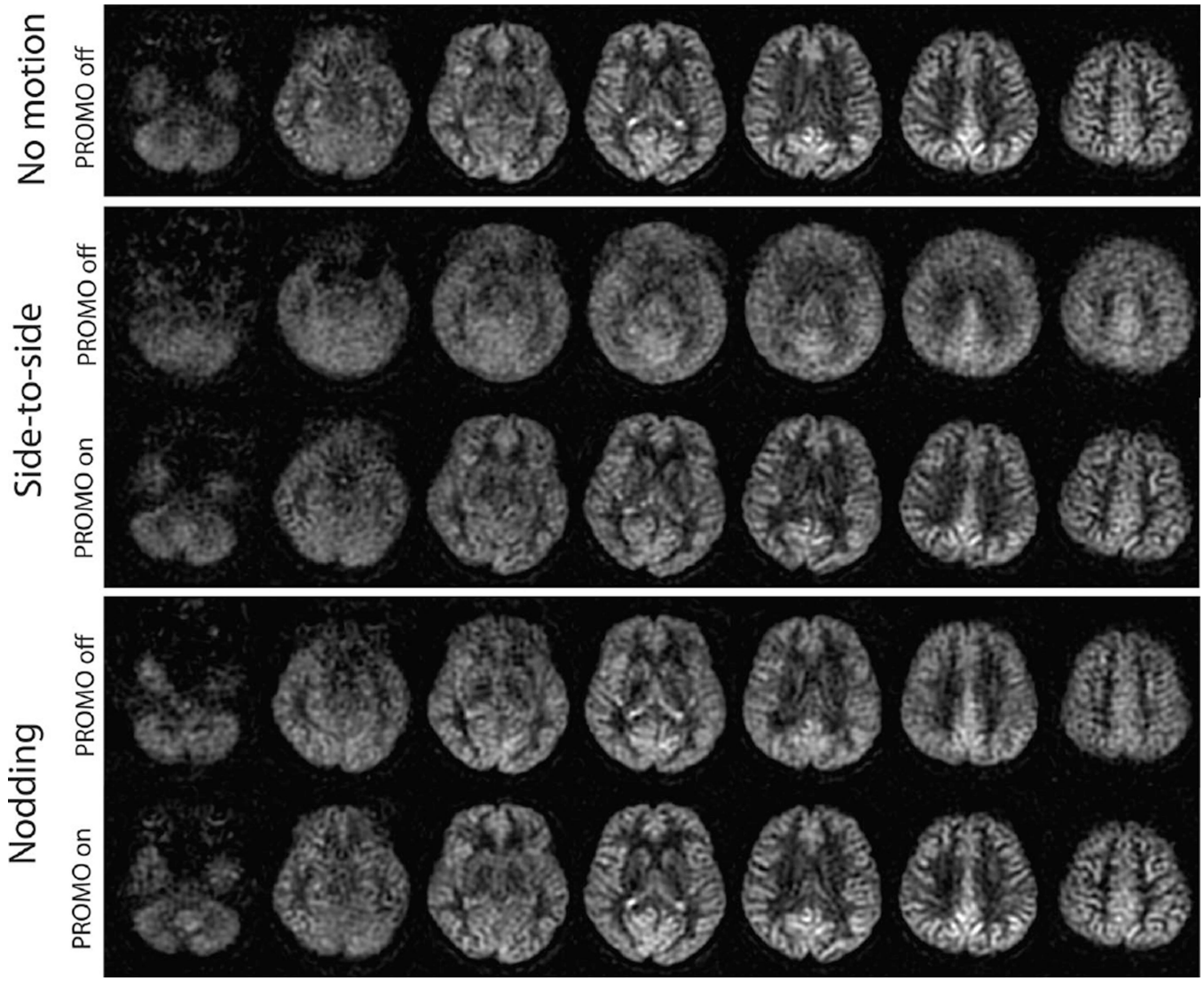


**FIG. 5.**

ASL images of selected slices from 3D whole brain acquired using PCASL with and without PROMO in a volunteer who performed controlled motions (side-to-side and nodding) repeatedly, and reference ASL images acquired without PROMO in the absence of any intended motion. For side-to-side motion, significant blurring was found in the ASL images without PROMO but was reduced substantially with PROMO. For nodding motion, there was no significant visible difference between ASL images with and without PROMO except for the slight blurring in the superior slices without PROMO.

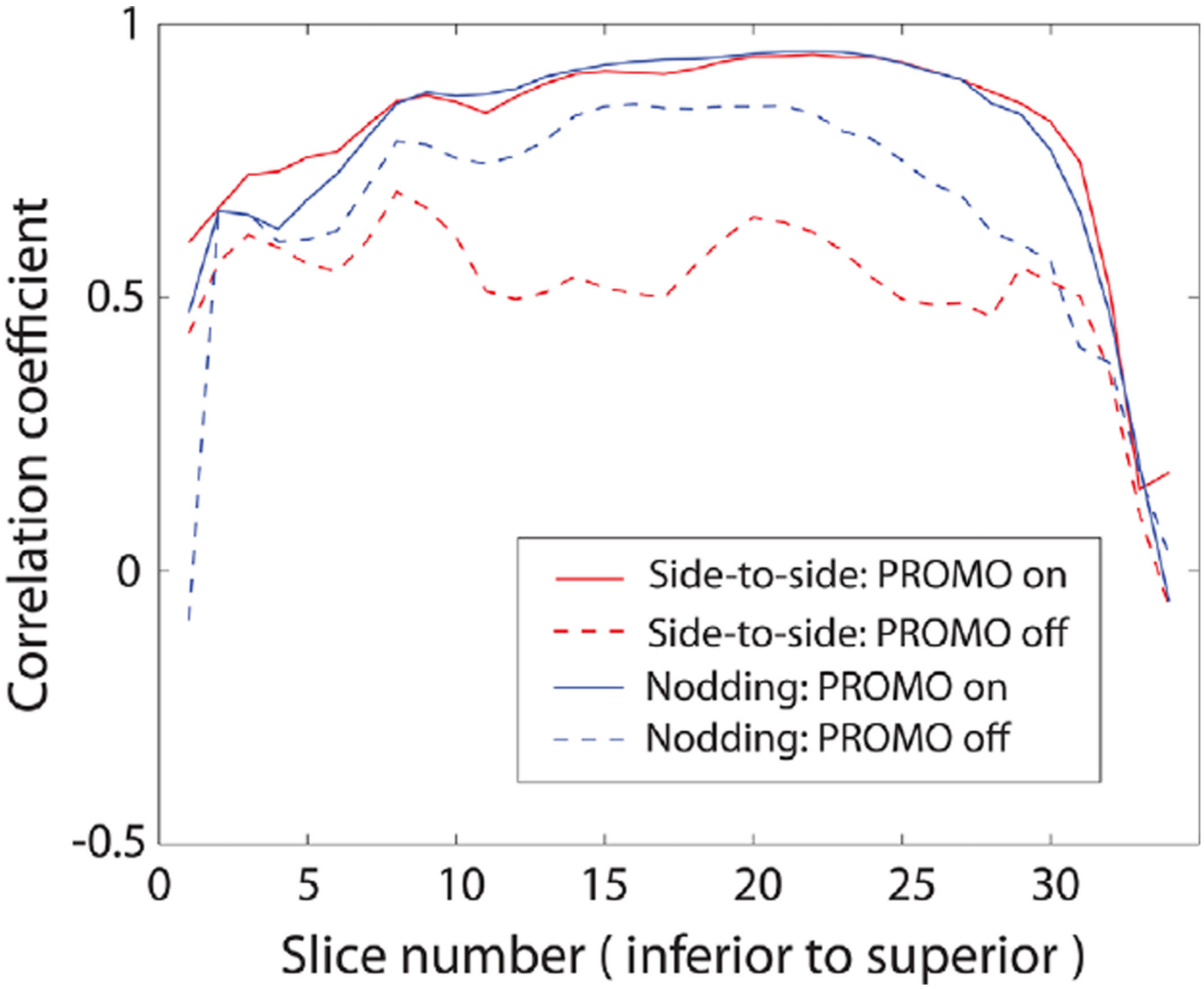


**FIG. 6.**

Correlation coefficients calculated for each slice between reference (no motion) images and the ASL images with or without PROMO for each motion type. [Color figure can be viewed in the online issue, which is available at wileyonlinelibrary.com.]

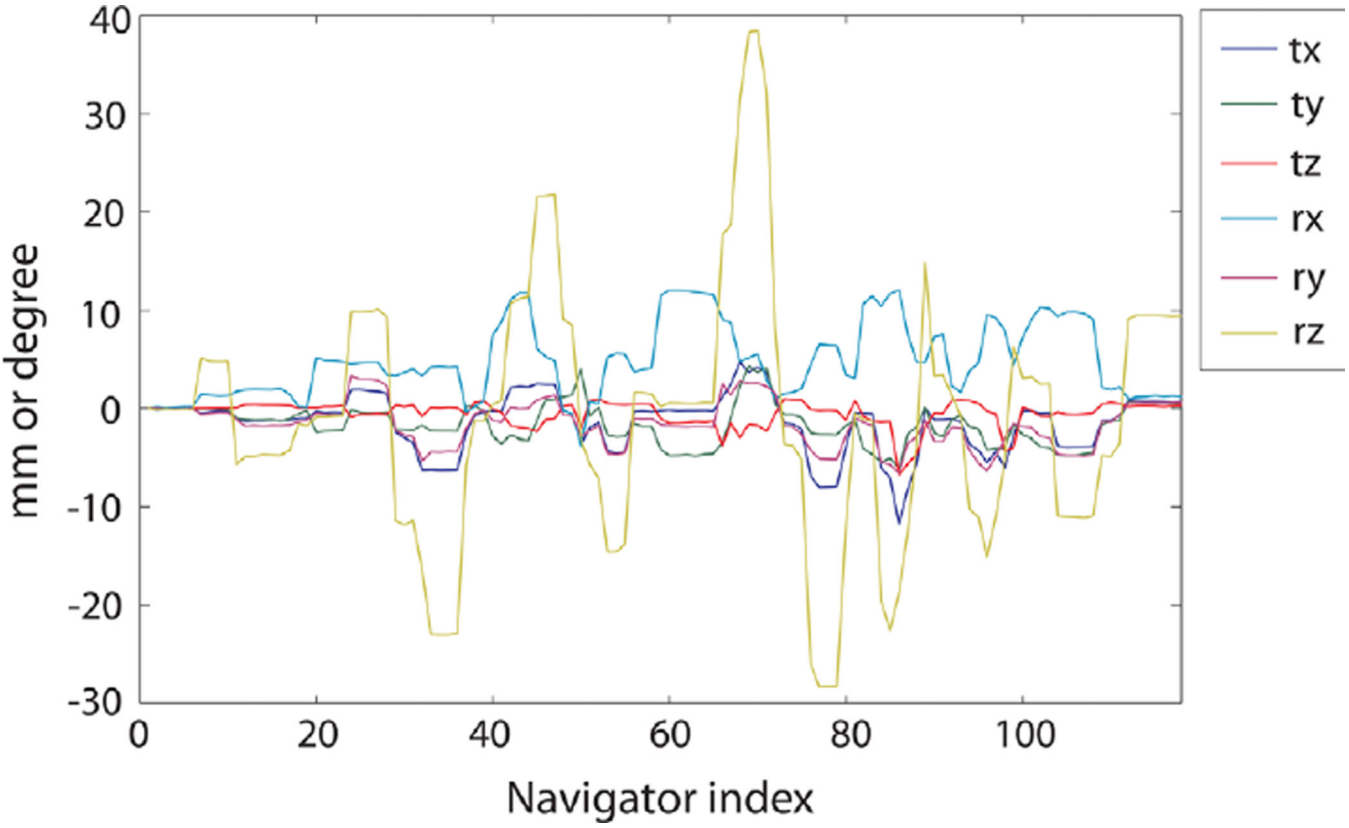


**FIG. 7.**

Motion parameters recorded in one representative volunteer during the interleaved scan where every TR was repeated twice with and without PROMO in the presence of random head motion. The two dominant motions were rotations along the *z*- and *x*-axes that correspond to side-to-side and nodding motions. [Color figure can be viewed in the online issue, which is available at wileyonlinelibrary.com.]

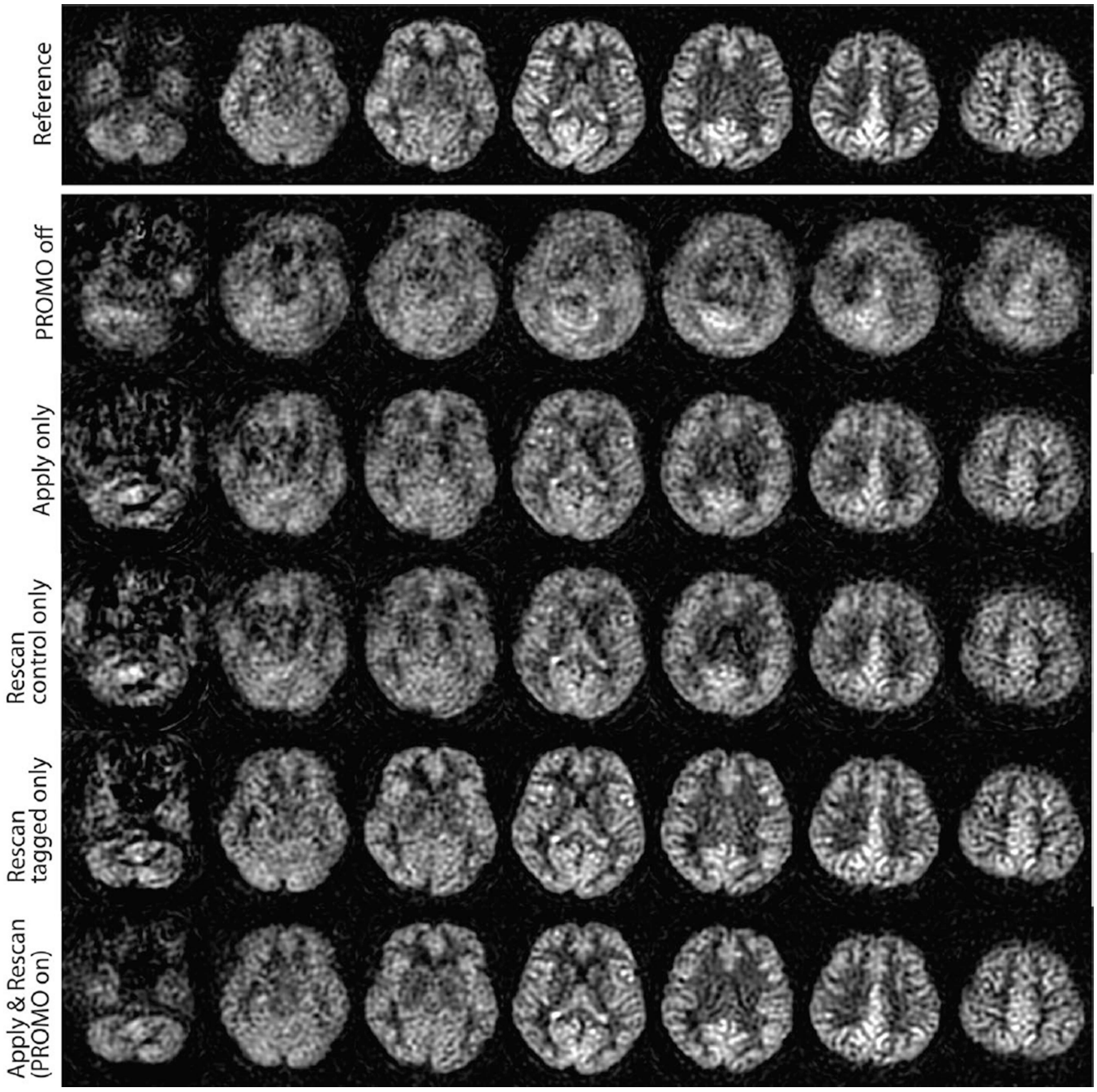


**FIG. 8.**

ASL images reconstructed from multiple combinations of the data acquired in the representative volunteer using interleaved PCASL-PROMO sequence in the presence of random motion. Reference: ASL images without PROMO in the absence of any intended motion. PROMO on/off: ASL images with/without PROMO. Apply only: ASL images with real-time updating of the coordinate system only (without rescanning of corrupted segments). Rescan tagged/control only: ASL images with real-time updating of the coordinate system and with rescanning (either tagged or control images only). ASL images

with apply only showed significantly reduced motion artifacts compared with images without PROMO, although residual blurring exists. Images in which rescanning was only applied to motion-corrupted tagged images were closer to the images with full PROMO correction than those with rescanning of motion-corrupted control images.

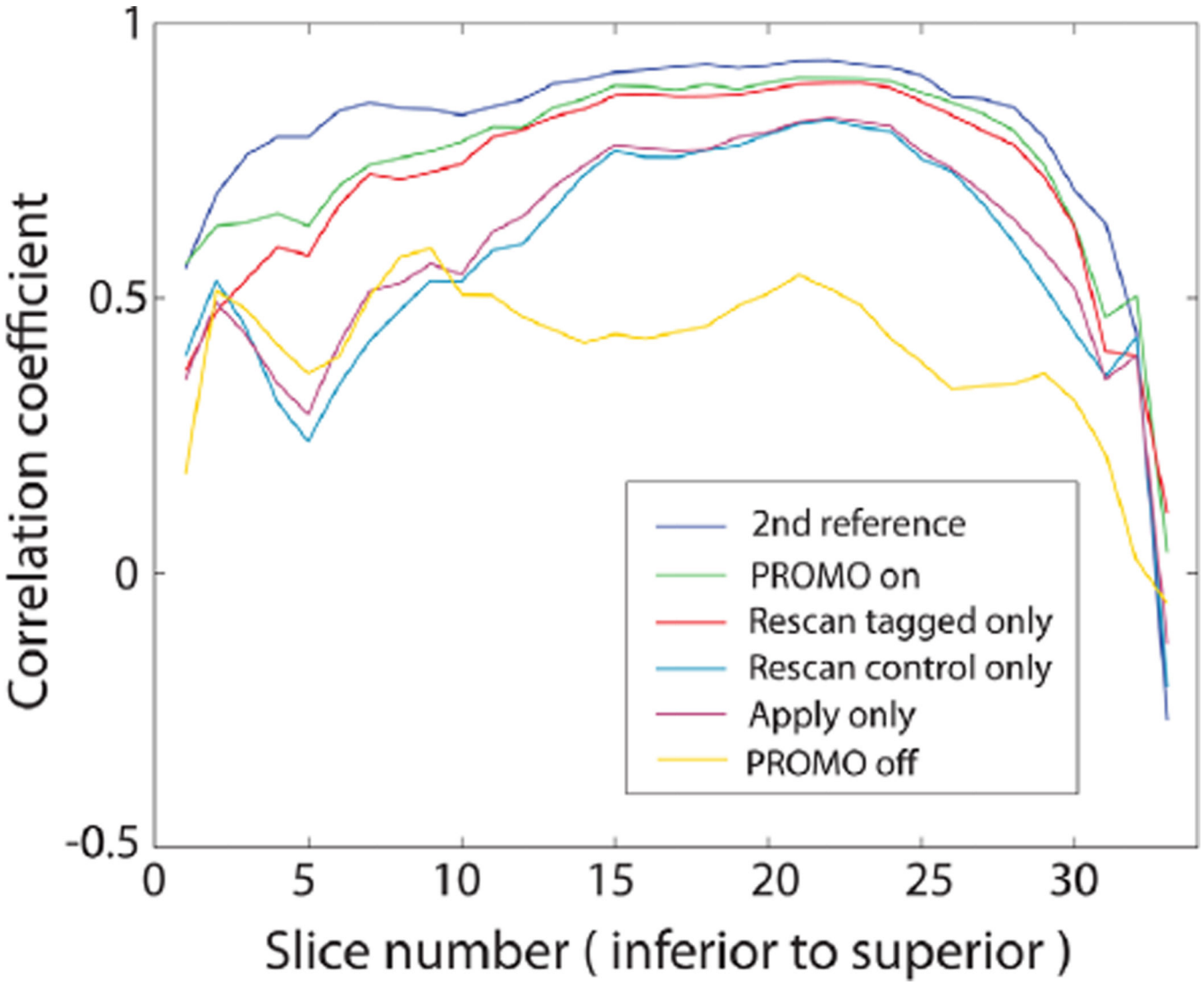


**FIG. 9.**

Correlation coefficients calculated for each slice between ASL images of each method and the first reference ASL images in the representative volunteer. Correlation coefficients between the first and second reference ASL images are also shown to provide the reference for the correlation coefficients.

## Table 1

Correlation Coefficients (CC) of the Whole 3D Volume with Respect to the Reference Images and Global CBF Measurements (in mL/100 g/min) in Gray Matter

| | Side-to-Side Motion | | Nodding Motion | |
|---|---|---|---|---|
| | **CC** | **CBF** | **CC** | **CBF** |
| PROMO on | 0.90 | 53.6 | 0.92 | 62.9 |
| PROMO off | 0.61 | 52.5 | 0.81 | 57.4 |

CBF of the reference ASL scan was 58.3 mL/100 g/min.

**Table 2**

Correlation Coefficients (CC) Between ASL Images of Each Reconstruction Method and the First Reference ASL Images and of Global CBF Measurements (in mL/100 g/min) in Gray Matter, Across Subjects

| | Second Reference | PROMO On | Rescan Tagged Only | Rescan Control Only | Apply Only | PROMO Off |
|---|---|---|---|---|---|---|
| CC | | | | | | |
| Mean ± SD | 0.85 ± 0.03 | 0.80 ± 0.05 | 0.74 ± 0.08 | 0.67 ± 0.07 | 0.69 ± 0.06 | 0.58 ± 0.06 |
| *P* | N/A | 0.036 | 0.030 | 0.005 | 0.006 | 0.001 |
| CBF | | | | | | |
| Mean ± SD | 56.0 ± 7.8 | 55.5 ± 7.8 | 58.8 ± 9.5 | 51.7 ± 9.2 | 54.2 ± 9.4 | 52.7 ± 9.1 |
| *P* | N/A | 0.606 | 0.245 | 0.120 | 0.426 | 0.094 |

Values are presented as the mean ± SD. *P* values were calculated using a *t* test with respect to the second reference scans.